Correspondence

Switch-and-Examine Diversity Over Arbitrarily Correlated Nakagami-m Fading Channels

George C. Alexandropoulos, *Student Member, IEEE*, P. Takis Mathiopoulos, *Senior Member, IEEE*, and Nikos C. Sagias, *Member, IEEE*

***Abstract*—The performance of switch-and-examine diversity (SED) over L arbitrarily correlated and not necessarily identically distributed Nakagami-m fading channels is studied. Analytical expressions for the distribution of the SED output signal-to-noise ratio (SNR) are obtained for the constant correlation model. For the most general case of arbitrary correlation, by assuming half-integer or integer values for the fading parameter m, analytical expressions for the distribution of the output SNR with $L \leq 3$ are derived. Moreover, for $L > 3$, analytical approximations for the output SNR are presented. The derived expressions are used to study the outage and average symbol error probability of SED receivers. Performance results obtained by numerical evaluation and verified by means of computer simulations show that the performance of the receivers under consideration is degraded with increasing branch correlation. Nevertheless, SED receivers outperform uncorrelated switch-and-stay diversity receivers, even when they operate under high branch correlation.**

***Index Terms*—Average bit error probability (ABEP), correlated fading, diversity techniques, multichannel receivers, Nakagami-m distribution, outage probability (OP), switched diversity.**

I. Introduction

Diversity techniques combat the destructive effects of multipath fading by means of multiple reception of the same information-bearing signal [1]. In practice, the vast majority of these techniques requires dedicated channel estimation and matched filtering for every diversity branch, which increases their implementation complexity [2], [3]. For reduced complexity implementations, a wide variety of switching-based diversity techniques has been proposed in the past (see, e.g., [4]–[9] and the references therein). Among these techniques, switch-and-stay diversity (SSD) [1]–[3], [5], [10], [11] and switch-and-examine diversity (SED) [4], [12] require estimation and processing of only one of the many diversity branches. These two diversity techniques are simple to implement at the expense of an attendant loss in performance [5]. Furthermore, they enable flexible designs since diversity can either be realized at the receiver or exploited at the transmitter's side [4]. To avoid switching during data transmission, both techniques are typically implemented in a discrete-time fashion (see, e.g., [2]–[5], for specific implementation designs). In particular, channel estimation and, when necessary, switching to alternative diversity branches are periodically performed during a guard period between two consecutive time slots for data transmission.

In multibranch SSD reception, the receiver switches to and stays with the next available diversity branch, regardless of its signal-to-noise ratio (SNR) when the instantaneous SNR on the current branch becomes unacceptable, i.e., lower than a certain switching threshold. For the SED, the combiner first examines the next branch's SNR and switches again only if this SNR is unacceptable. When switched diversity is used at the transmitter, the downlink channel corresponding to the selected branch is monitored either through a feedback channel or by using a time-division duplex protocol that capitalizes on the reciprocity of the channel [4]. The importance of using these two low-complexity diversity techniques is well known, particularly in practical cost-stringent applications, e.g., for power- and/or size-limited mobile terminals, such as mobile handsets [13], [14], where correlated fading is usually present [1], [15]–[28]. On the one hand, multibranch SSD has been studied for various not necessarily identically distributed (i.d.) and/or arbitrarily correlated fading channels [4], [5], [10], [23]. Interestingly, it has been established that its performance does not improve for more than two diversity branches [4]. On the other hand, despite the fact that, in general, SED performance improves with increasing number of diversity branches [4], [12], to the best of our knowledge, multibranch SED has been studied so far only for independent and i.d. fading channels.

In this paper, we study the performance of multibranch SED over L arbitrarily correlated and not necessarily i.d. Nakagami-m fading channels. For the constant correlation model, analytical expressions in the form of infinite series for the cumulative distribution function (CDF) and the probability density function (PDF) of the SED output SNR are derived. Assuming arbitrary correlation and half-integer or integer values of the fading parameter m, analytical expressions and approximations in infinite series form are derived for the distribution of the SED output SNR, with $L \leq 3$ and $L > 3$, respectively. These expressions are used to study the outage probability (OP) and average symbol error probability (ASEP) of multibranch SED. The analysis and the theoretical performance results obtained are verified through comparisons with equivalent computer simulation performance evaluation results.

The remainder of this paper is organized as follows: In Section II, analytical expressions for the distribution of the SED output SNR are derived, whereas in Section III, the performance analysis of multibranch SED receivers is presented. Section IV presents numerical and computer simulation performance evaluation results, and Section V contains the conclusions.

II. Output Signal-to-Noise Ratio Statistics

Let us consider a diversity system with L correlated branches receiving digitally modulated signals transmitted over a slow-varying and frequency-nonselective Nakagami-m fading channel. The baseband signal received at the ℓth[1] diversity branch can be expressed as

$$R_\ell(t) = \alpha_\ell \exp(-j\phi_\ell)s(t) + n_\ell(t), \qquad 0 \leq t < T_s \qquad (1)$$

[1]Unless otherwise stated, indexes ℓ and i, which will be introduced later, take values $0, 1, \ldots, L-1$. Furthermore, indexes r and s, which will be introduced later on take values $0, 1, \ldots, L-2$ and $1, 2, \ldots, L-1$, respectively.

Manuscript received December 19, 2008; revised July 15, 2009 and October 19, 2009. First published January 22, 2010; current version published May 14, 2010. This work was performed within the framework of the Network of Excellence in Wireless COMmunications NEWCOM++ under Contract 216715, which was supported by the European Committee under the FP7 Research Program. The review of this paper was coordinated by Prof. J. Wu.

G. C. Alexandropoulos is with the Department of Computer Engineering and Informatics, University of Patras, 26500 Rio-Patras, Greece, and also with the Wireless Communications Laboratory, Institute of Informatics and Telecommunications, National Centre for Scientific Research–"Demokritos," 15310 Athens, Greece (e-mail: alexandg@ieee.org).

P. T. Mathiopoulos is with the Institute for Space Applications and Remote Sensing, National Observatory of Athens, 15236 Athens, Greece (e-mail: mathio@space.noa.gr).

N. C. Sagias is with the Department of Telecommunications Science and Technology, University of Peloponnese, 22100 Tripolis, Greece (e-mail: nsagias@ieee.org).

Digital Object Identifier 10.1109/TVT.2010.2041016

where $s(t)$ is the transmitted complex information-bearing signal with average symbol energy E_s and symbol duration T_s, α_ℓ is the fading envelope of the ℓth diversity branch, and ϕ_ℓ is its random phase. Furthermore, $n_\ell(t)$ is the additive white Gaussian noise (AWGN) of the ℓth diversity branch having single-sided power spectral density N_0. The amplitude α_ℓ is assumed to follow the Nakagami-m distribution with marginal PDF $f_{\alpha_\ell}(\alpha) = 2\alpha^{2m-1}/[\,\Gamma(m)\Omega_\ell^m\,]\exp(-\alpha^2/\Omega_\ell)$, where $\Gamma(\cdot)$ is the Gamma function [29, eq. (8.310/1)], $\Omega_\ell = \mathbb{E}\langle\alpha_\ell^2\rangle/m$ is a parameter related to the average fading power, $\mathbb{E}\langle\cdot\rangle$ denotes expectation, and $m \geq 1/2$. For ϕ_ℓ, we make the usual assumptions that it is uniformly distributed over the range $[0, 2\pi)$ and that it can be estimated and, thus, canceled at the receiver. Moreover, the AWGN between diversity branches is assumed to be uncorrelated and statistically independent of the received digitally modulated signal.

A. CDF

Let $\mathbf{x}^{(i,\ell)}$ denote the $(\ell+1)$-dimensional row vector $\mathbf{x}^{(i,\ell)} = [\,x_{(i-\ell)_L} \quad x_{(i-\ell+1)_L} \quad \cdots \quad x_i\,]$, with $(i-\ell)_L$ being the $(i-\ell)$ modulo L operation. Following this notation, let $\mathbf{g}^{(L-1,L-1)} = [\,g_0 \quad g_1 \quad \cdots \quad g_{L-1}\,]$, where $g_\ell = E_s\alpha_\ell^2/N_0$ is a vector with the instantaneous received SNRs per symbol, and $\overline{\mathbf{g}}^{(L-1,L-1)} = [\,\overline{g}_0 \quad \overline{g}_1 \quad \cdots \quad \overline{g}_{L-1}\,]$ is a vector denoting its average value. With SED reception, if the received instantaneous SNR of the selected branch becomes lower than a predetermined switching threshold g_T, the combiner examines the next branch's SNR and switches again only if this SNR is unacceptable [4]. In case where the instantaneous SNR of all L branches is lower than g_T, the combiner either uses the last examined branch or switches back to the first branch for the next transmission slot. Based on this mode of operation and using [4, eq. (28)], the CDF of the SED output SNR can mathematically be expressed as in (2), shown at the bottom of the page, where p_i is the probability that the system uses the ith antenna branch, $F_{g_i}(g)$ is the marginal CDF of g_i [1, Tab. 2.2], and $F_{\mathbf{g}^{(i,\ell)}}[\mathbf{g}^{(i,\ell)}]$, $\ell \geq 1$ is the joint CDF of $\mathbf{g}^{(i,\ell)}$. In general, the elements of $\mathbf{g}^{(L-1,L-1)}$ can arbitrarily be correlated with the power correlation matrix (CM) $\mathbf{\Sigma}_{\mathbf{g}^{(L-1,L-1)}} \in \Re^{L\times L}$. This matrix is symmetric, positive definite, and given by $\mathbf{\Sigma}^{j,k}_{\mathbf{g}^{(L-1,L-1)}} \equiv 1$ for $j = k$, with $j,k = 1,2,\ldots,L$ and $\mathbf{\Sigma}^{j,k}_{\mathbf{g}^{(L-1,L-1)}} \equiv \rho_{j,k}$ for $j \neq k$, where $\rho_{j,k} \in [0,1)$ is the power correlation coefficient between g_{j-1} and g_{k-1} [1, eq. (9.195)]. Using $\mathbf{\Sigma}_{\mathbf{g}^{(L-1,L-1)}}$, the CM of $\mathbf{g}^{(r,s)}$, i.e., $\mathbf{\Sigma}_{\mathbf{g}^{(r,s)}}$, is constructed as $\mathbf{\Sigma}^{n,q}_{\mathbf{g}^{(r,s)}} = \rho_{v_n+1,v_q+1}$, where $n,q = 1,2,\ldots,s+1$ and $v_n = (r-s+n-1)_L$. For example, to evaluate $F_{\mathbf{g}^{(1,2)}}[\mathbf{g}^{(1,2)}]$ required in (2) for $L \geq 3$, $\mathbf{\Sigma}_{\mathbf{g}^{(1,2)}}$ is constructed from $\mathbf{\Sigma}_{\mathbf{g}^{(L-1,L-1)}}$ as $\mathbf{\Sigma}^{1,2}_{\mathbf{g}^{(1,2)}} = \rho_{L,1}$, $\mathbf{\Sigma}^{1,3}_{\mathbf{g}^{(1,2)}} = \rho_{L,2}$, and $\mathbf{\Sigma}^{2,3}_{\mathbf{g}^{(1,2)}} = \rho_{1,2}$.

Clearly, to obtain analytical expressions for $F_{g_{\text{sed}}}(g)$, expressions for the p_i's and $F_{\mathbf{g}^{(i,s)}}[\mathbf{g}^{(i,s)}]$ are necessary. Starting with the p_i's and similar to [5], by modeling the SED receiver mode of operation as an L-state Markov chain, the p_i's represent the elements of its stationary distribution $\mathbf{p}^{(L-1,L-1)} = [\,p_0 \quad p_1 \quad \cdots \quad p_{L-1}\,]$. The transition probabilities $P_{i,\ell}$'s of this chain's transition matrix $\mathbf{P} = [P_{i,\ell}]$ are given by [4, eq. (29)], and $\mathbf{p}^{(L-1,L-1)}$ can be derived using

$$\sum_{i=0}^{L-1} p_i = 1 \tag{3}$$

$$\mathbf{p}^{(L-1,L-1)} = \mathbf{p}^{(L-1,L-1)}\,\mathbf{P}. \tag{4}$$

The preceding two equations can be used to obtain the p_i's for a triple-branch SED receiver as

$$p_0 = \frac{xz}{z(x+y)+wx} \tag{5a}$$

$$p_1 = \frac{y}{x}p_0 \tag{5b}$$

$$p_2 = \frac{w}{z}p_0 \tag{5c}$$

where $x = (1-P_{1,1})z - P_{1,2}P_{2,1}$, $y = P_{0,1}z + P_{0,2}P_{2,1}$, $z = (1-P_{2,2})$, and $w = P_{0,2} + yP_{1,2}/x$.

As far as $F_{\mathbf{g}^{(i,s)}}[\mathbf{g}^{(i,s)}]$ is concerned, in the past, analytical expressions have been proposed for various forms of the CM $\mathbf{\Sigma}_{\mathbf{g}^{(i,s)}}$. Possibly, the first paper published in the open technical literature that dealt with the derivation of an expression for the exact $F_{\mathbf{g}^{(i,\ell)}}[\mathbf{g}^{(i,s)}]$ proposing a multiple series of generalized Laguerre polynomials as a solution was [30]. However, such expression is not useful for $s \geq 2$, i.e., more than two random variables, since it not only becomes prohibitively complex but also has very poor convergence properties [20]. Hence, simpler expressions have been introduced, considering special forms of the CM $\mathbf{\Sigma}_{\mathbf{g}^{(i,s)}}$ (see, e.g., [15], [18], [21], [22], [26], and [27]). In particular, for Nakagami-m fading, $F_{\mathbf{g}^{(i,1)}}[\mathbf{g}^{(i,1)}]$ has been obtained from [15, eq. (3)], whereas $F_{\mathbf{g}^{(i,2)}}[\mathbf{g}^{(i,2)}]$ has been derived from [21, eq. (6)] or [27, eq. (11)] for $m = 1$ (i.e., for Rayleigh fading) and [22, eq. (20)] or [27, eq. (8)] for integer or half-integer $m \geq 3/2$, respectively. For the special case of $w_{1,4}^{(i,3)} = 0$, with $\mathbf{W}_{\mathbf{g}^{(i,s)}} = [w_{j,k}^{(i,s)}]$ being the inverse of the Gaussian CM $\mathbf{\Sigma}^G_{\mathbf{g}^{(i,s)}} = \sqrt{\mathbf{\Sigma}_{\mathbf{g}^{(i,s)}}}$, $F_{\mathbf{g}^{(i,3)}}[\mathbf{g}^{(i,3)}]$ has been obtained from [21, eq. (19)] for $m = 1$ and [22, eq. (15)] for integer or half-integer $m \geq 3/2$. For the constant correlation model [1, Ch. 9], i.e., $\mathbf{\Sigma}^{j,k}_{\mathbf{g}^{(i,s)}} = \rho\ \forall\, j \neq k$, $F_{\mathbf{g}^{(i,s)}}[\mathbf{g}^{(i,s)}]$ has been obtained in [26, eq. (7)], whereas for the exponential one, i.e., $\mathbf{\Sigma}^{j,k}_{\mathbf{g}^{(i,s)}} = \rho^{|j-k|}\ \forall\, j \neq k$, where $|\cdot|$ denotes absolute value, it has been derived for i.d. fading, i.e., $\overline{\mathbf{g}}^{(s+1,s+1)} = \overline{g}$, using [18, eq. (6)]. For the arbitrary correlation model and assuming i.d. fading, a tight upper bound and an accurate approximation for the exact $F_{\mathbf{g}^{(i,s)}}[\mathbf{g}^{(i,s)}]$ have been obtained in [25, eq. (21)] and using the analysis of [19], respectively.

In an effort to obtain a unified representation for $F_{\mathbf{g}^{(i,s)}}[\mathbf{g}^{(i,s)}]$ that includes the aforementioned expressions as special cases, the

$$F_{g_{\text{sed}}}(g) = \begin{cases} \sum_{i=0}^{L-1} p_i\, F_{\mathbf{g}^{(i,L-1)}}(g_T,\ldots,g_T,g), & g < g_T \\ \sum_{i=0}^{L-1} \Big\{ p_i \left[F_{g_i}(g) - F_{g_i}(g_T) + F_{\mathbf{g}^{(L-1,L-1)}}(g_T,\ldots,g_T,g_T)\right] \\ \qquad + p_{(i-1)_L} \left[F_{\mathbf{g}^{(i,1)}}(g_T,g) - F_{\mathbf{g}^{(i,1)}}(g_T,g_T)\right] \\ \qquad + p_{(i-2)_L} \left[F_{\mathbf{g}^{(i,2)}}(g_T,g_T,g) - F_{\mathbf{g}^{(i,2)}}(g_T,g_T,g_T)\right] + \cdots \\ \qquad + p_{(i-L+1)_L} \left[F_{\mathbf{g}^{(i,L-1)}}(g_T,\ldots,g_T,g) - F_{\mathbf{g}^{(i,L-1)}}(g_T,\ldots,g_T,g_T)\right] \Big\}, & g \geq g_T \end{cases} \tag{2}$$

following *novel* generic expression is proposed:

$$F_{\mathbf{g}^{(i,s)}}\left[\mathbf{g}^{(i,s)}\right] = \sum_{k_1,k_2,\ldots,k_U=0}^{\infty} \mathcal{A}\left[\mathbf{\Sigma}_{\mathbf{g}^{(i,s)}}, \{k_u\}_{u=1}^{U}\right] \times \prod_{j=1}^{s+1} \gamma\left[\kappa_j, \xi_j \frac{g_{(i+j-s-1)_{s+1}}}{\overline{g}_{(i+j-s-1)_{s+1}}}\right] \quad (6)$$

where $\gamma(\cdot,\cdot)$ is the lower incomplete Gamma function [29, eq. (8.350/1)]; U is an integer constant; κ_j and ξ_j, where j takes values $1, 2, \ldots, s+1$, are positive real parameters; and $\mathcal{A}[\mathbf{\Sigma}_{\mathbf{g}^{(i,s)}}, \{k_u\}_{u=1}^{U}]$ is a function of $\mathbf{\Sigma}_{\mathbf{g}^{(i,s)}}$ and $\{k_u\}_{u=1}^{U}$.

Although exact numerical evaluation of the right-hand side (RHS) of (6) requires U summations of an infinite number of terms, in practice, U minimum numbers of terms $N_1, N_2, \ldots, N_U$ are selected in the summations leading to a certain accuracy. Similar to [21], by using the inequality $\gamma(\alpha, x) \leq \Gamma(\alpha)$, the truncation error T_e of the RHS of (6) can be upper bounded as

$$\begin{aligned}|T_e| \leq & \sum_{k_1=N_1}^{\infty} \sum_{k_2,k_3,\ldots,k_U=0}^{\infty} \mathcal{B}\left(\{k_u\}_{u=1}^{U}\right) \\ & + \sum_{k_1=0}^{N_1-1} \sum_{k_2=N_2}^{\infty} \sum_{k_3,k_4,\ldots,k_U=0}^{\infty} \mathcal{B}\left(\{k_u\}_{u=1}^{U}\right) + \cdots \\ & + \sum_{k_1=0}^{N_1-1} \sum_{k_2=0}^{N_2-1} \cdots \sum_{k_{U-1}=0}^{N_{U-1}-1} \sum_{k_U=N_U}^{\infty} \mathcal{B}\left(\{k_u\}_{u=1}^{U}\right) \end{aligned} \quad (7)$$

where

$$\mathcal{B}\left(\{k_u\}_{u=1}^{U}\right) = \mathcal{A}\left[\mathbf{\Sigma}_{\mathbf{g}^{(i,s)}}, \{k_u\}_{u=1}^{U}\right] \prod_{j=1}^{s+1} (\kappa_j - 1)!. \quad (8)$$

It is useful to note that a tighter bound on the RHS of (6) can be obtained using the methodology in [15, Sec. III] at the expense of more mathematical rigor.

The specific expression the function $\mathcal{A}[\mathbf{\Sigma}_{\mathbf{g}^{(i,s)}}, \{k_u\}_{u=1}^{U}]$ takes, the values of U, and the parameters κ_j and ξ_j strongly depend on m and $\mathbf{\Sigma}_{\mathbf{g}^{(i,s)}}$. Next, we present examples where the use of (6) leads to previously known expressions for $F_{\mathbf{g}^{(i,s)}}[\mathbf{g}^{(i,s)}]$ that have been derived, assuming certain correlation models.

Constant Correlation Model: An exact expression for $F_{\mathbf{g}^{(i,s)}}[\mathbf{g}^{(i,s)}]$ has been obtained by substituting in (6)

$$U = s+1 \quad (9a)$$

$$\mathcal{A}\left[\mathbf{\Sigma}_{\mathbf{g}^{(i,s)}}, \{k_u\}_{u=1}^{s+1}\right] = \frac{(1-\sqrt{\rho})^m \Gamma\left(m + \sum_{j=1}^{s+1} k_j\right)}{\Gamma(m)(1+s\sqrt{\rho})^{m+\sum_{j=1}^{s+1} k_j}} \times \frac{\rho^{1/2\sum_{j=1}^{s+1} k_j}}{\prod_{j=1}^{s+1} k_j! \Gamma(k_j+m)} \quad (9b)$$

$$\kappa_j = k_j + m \quad (10a)$$

$$\xi_j = \frac{m}{(1-\sqrt{\rho})}. \quad (10b)$$

This expression is identical to a previously known expression for the constant correlation model [26, eq. (7)].

Arbitrary Correlation Model: For $L = 2$, an exact expression for $F_{\mathbf{g}^{(i,1)}}[\mathbf{g}^{(i,1)}]$ has been obtained by substituting in (6)

$$U = 1 \quad (11a)$$

$$\mathcal{A}\left[\mathbf{\Sigma}_{\mathbf{g}^{(i,1)}}, k_1\right] = \frac{(1-\sqrt{\varrho_i})^m \varrho_i^{\kappa_1/2}}{k_1! \Gamma(m) \Gamma(\kappa_1)} \quad (11b)$$

where $\varrho_i = \rho_{1+(i-1)_L, 1+i}$, and

$$\kappa_j = k_1 + m \quad (12a)$$

$$\xi_j = \frac{m}{(1-\sqrt{\varrho_i})}. \quad (12b)$$

Although, due to space limitations, this expression will not be presented here, it can easily be derived from [15, eq. (3)] using a standard random variable transformation.

For $L = 3$, an exact expression for $F_{\mathbf{g}^{(i,2)}}[\mathbf{g}^{(i,2)}]$ has been obtained by substituting in (6) $U = 4$, $\mathcal{A}[\mathbf{\Sigma}_{\mathbf{g}^{(i,2)}}, \{k_u\}_{u=1}^{4}]$ as in (13), shown at the bottom of the page, where $\det(\cdot)$ denotes the determinant, ν_{k_4} is the Neumann factor ($\nu_0 = 1$ and $\nu_t = 2$ for $t = 1, 2, \ldots$), and $\psi_{i,j} = |w_{i,j}^{(i,2)}|^2 [w_{i,i}^{(i,2)} w_{j,j}^{(i,2)}]^{-1}$

$$\kappa_1 = \begin{cases} k_1 + k_3 + k_4 + 1, & m = 1 \\ k_1 + k_2 + k_4 + m, & m \geq 3/2 \end{cases} \quad (14a)$$

$$\kappa_2 = \begin{cases} k_1 + k_2 + k_4 + 1, & m = 1 \\ k_1 + k_3 + k_4 + m, & m \geq 3/2 \end{cases} \quad (14b)$$

$$\kappa_3 = k_2 + k_3 + k_4 + m \quad (14c)$$

$$\xi_j = m w_{j,j}^{(i,2)}. \quad (14d)$$

Although, due to space limitations, this expression is not presented here, it can also be easily derived from [21, eq. (19)] for $m = 1$ and [22, eq. (15)] for integer or half-integer $m \geq 3/2$.

For $L > 3$ and i.d. fading, i.e., $\overline{g}_{(i+j-n-1)_{n+1}} = \overline{g}$, $n = 3, 4, \ldots, L-1$, analytical expressions and approximations for the exact $F_{\mathbf{g}^{(i,n)}}[\mathbf{g}^{(i,n)}]$ can be obtained by substituting in (6)

$$U = n \quad (15a)$$

$$\mathcal{A}\left(\mathbf{Z}, \{k_u\}_{u=1}^{n}\right) = \frac{\det(\mathbf{Z})^m \prod_{j=1}^{n} z_{j,j+1}^{2k_j} \Big/ \left[k_j! \Gamma(k_j+m)\right]}{\Gamma(m) z_{1,1}^{k_1+m} z_{n+1,n+1}^{k_n+m} \prod_{j=2}^{n} z_{j,j}^{k_{j-1}+k_j+m}} \quad (15b)$$

where $\mathbf{Z} = [z_{j,k}] \in \Re^{(n+1)\times(n+1)}$, and

$$\kappa_1 = k_1 + m \quad (16a)$$

$$\kappa_p = k_{p-1} + k_p + m, \qquad p = 2, 3, \ldots, L-1 \quad (16b)$$

$$\kappa_{n+1} = k_n + m \quad (16c)$$

$$\xi_j = m z_{j,j}. \quad (16d)$$

For the special case of $\mathbf{W}_{\mathbf{g}^{(i,n)}}$ being tridiagonal, e.g., for an exponential CM $\mathbf{\Sigma}_{\mathbf{g}^{(i,n)}}$, an analytical expression for the exact $F_{\mathbf{g}^{(i,n)}}[\mathbf{g}^{(i,n)}]$ can be obtained by substituting (15) and (16) for $\mathbf{Z} = \mathbf{W}_{\mathbf{g}^{(i,n)}}$ in (6). Similar to the previous cases, it can easily be verified that this

$$\mathcal{A}\left[\mathbf{\Sigma}_{\mathbf{g}^{(i,2)}}, \{k_u\}_{u=1}^{4}\right] = \begin{cases} \det\left[\mathbf{W}_{\mathbf{g}^{(i,2)}}\right] \frac{\nu_{k_4} (-1)^{k_4} \psi_{1,2}^{k_1+k_4/2} \psi_{2,3}^{k_2+k_4/2} \psi_{3,1}^{k_3+k_4/2}}{\prod_{\ell=1}^{3} k_\ell! (k_\ell+k_4)! w_{\ell,\ell}^{(i,2)}}, & m = 1 \\ \det\left[\mathbf{W}_{\mathbf{g}^{(i,2)}}\right]^m \frac{(-1)^{k_4} (m+k_4-1) \binom{2m+k_4-3}{2m-3} \left[w_{1,2}^{(i,2)}\right]^{2k_1+k_4} \left[w_{1,3}^{(i,2)}\right]^{2k_2+k_4} \left[w_{2,3}^{(i,2)}\right]^{2k_3+k_4}}{(m-1) \prod_{\ell=1}^{3} k_\ell! \Gamma(k_\ell+m+k_4) \left[w_{\ell,\ell}^{(i,2)}\right]^{\kappa_\ell}}, & m \geq 3/2 \end{cases} \quad (13)$$

expression can also be derived from [18, eq. (6)] in a straightforward way; thus, it will not be repeated here. For an arbitrary CM $\mathbf{\Sigma}_{\mathbf{g}^{(i,n)}}$, again, substituting (15) and (16) for $\mathbf{Z} = \mathbf{C}^{-1}_{\mathbf{g}^{(i,n)}}$ in (6), where $\mathbf{C}_{\mathbf{g}^{(i,n)}}$ is a Green's matrix with the elements being the closest possible values to the entries of $\mathbf{\Sigma}_{\mathbf{g}^{(i,n)}}$, yields an approximation for $F_{\mathbf{g}^{(i,n)}}[\mathbf{g}^{(i,n)}]$. It is noted that the same expression can also be easily derived using the analysis in [19].

B. PDF

Substituting (6) in (2) and after differentiation, the PDF of the SED output SNR can be expressed as

$$f_{g_{\rm sed}}(g) = \begin{cases} \sum_{i=0}^{L-1} \sum_{k_1,k_2,\ldots,k_U=0}^{\infty} p_i \xi_L^{\kappa_L} \\ \quad \times \mathcal{A}\left[\mathbf{\Sigma}_{\mathbf{g}^{(i,L-1)}}, \{k_u\}_{u=1}^{U}\right] \mathcal{C}_{L-1}(g_T) \\ \quad \times H(\kappa_L, \xi_L, g), & g < g_T \\ \sum_{i=0}^{L-1} \left\{ p_i \frac{(m/\overline{g}_i)^m}{\Gamma(m)} H\left(m, \frac{m}{\overline{g}_i}, g\right) \right. \\ \quad + \sum_{s=1}^{L-1} \sum_{k_1,k_2,\ldots,k_U=0}^{\infty} p_{(i-s)_L} \\ \quad \times \xi_{s+1}^{\kappa_{s+1}} \mathcal{A}\left[\mathbf{\Sigma}_{\mathbf{g}^{(i,s)}}, \{k_u\}_{u=1}^{U}\right] \\ \quad \left. \times \mathcal{C}_s(g_T) H(\kappa_{s+1}, \xi_{s+1}, g) \right\}, & g \geq g_T \end{cases} \tag{17}$$

where $\mathcal{C}_s(g_T) = \prod_{j=1}^{s} \gamma[\kappa_j, \xi_j g_T / \overline{g}_{(i+j-s-1)_{s+1}}]$, and function $H(a,b,g)$ is defined as

$$H(a,b,g) \triangleq g^{a-1} \exp(-bg) \tag{18}$$

with a and b being positive real constants.

Next, first, considering a constant CM $\mathbf{\Sigma}_{\mathbf{g}^{(L-1,L-1)}}$, the procedure that will lead to the derivation of *novel* analytical expressions for the exact $f_{g_{\rm sed}}(g)$ will be highlighted. Second, for the most general case of an arbitrary CM $\mathbf{\Sigma}_{\mathbf{g}^{(L-1,L-1)}}$, we have obtained the following: 1) for $L \leq 3$, *novel* analytical expressions for the exact $f_{g_{\rm sed}}(g)$ and 2) for $L \geq 4$, approximations for $f_{g_{\rm sed}}(g)$. Although, due to space limitations, the latter expressions will not be shown here, the steps leading to their derivation will also be highlighted.

Constant Correlation: For a constant $\mathbf{\Sigma}_{\mathbf{g}^{(L-1,L-1)}}$, the $\mathbf{\Sigma}_{\mathbf{g}^{(i,s)}}$'s are also constant CMs. By substituting (9) and (10) in (17), an analytical expression for the exact $f_{g_{\rm sed}}(g)$ is obtained, as in (19), shown at the bottom of the page. For $L = 2$, this expression is identical with [4] since dual-branch SED and dual-branch SSD have identical performances [4].

Arbitrary Correlation: Similar to the derivation of (19), substituting (11)–(14) in (6) and then in (17) yields an analytical expression for the exact $f_{g_{\rm sed}}(g)$ for $L \leq 3$. Again, for $L = 2$, this expression agrees with [4, eq. (11)]. For $L \geq 4$, substituting (11)–(14) in (6) and (15) and (16) with $\mathbf{Z} = \mathbf{W}_{\mathbf{g}^{(i,n)}}$ when $\mathbf{W}_{\mathbf{g}^{(i,n)}}$ is tridiagonal and with $\mathbf{Z} = \mathbf{C}^{-1}_{\mathbf{g}^{(i,n)}}$ for arbitrary forms of $\mathbf{W}_{\mathbf{g}^{(i,n)}}$'s yields an analytical approximation for the exact $f_{g_{\rm sed}}(g)$, which can be found in [28].

III. Performance Analysis

The previously described formulas will be used to obtain analytical expressions for the performance of multibranch SED receivers operating over arbitrarily correlated and not necessarily i.d. Nakagami-m fading channels.

A. OP

The OP $P_{\rm out}$ is defined as the probability that the SED output SNR falls below a given outage threshold $g_{\rm th}$. This probability can easily be obtained by setting $g = g_{\rm th}$ in (2), yielding

$$P_{\rm out}(g_{\rm th}) = F_{g_{\rm sed}}(g_{\rm th}). \tag{20}$$

For arbitrarily correlated triple-branch and constantly correlated multibranch SED receivers, (20) provides an analytical expression for the exact $P_{\rm out}$, whereas for $L \geq 4$ and arbitrarily correlated i.d. fading, (20) provides an analytical approximation.

B. ASEP

The ASEP $\overline{P}_s$ is obtained by averaging the conditional symbol error probability $P_s(g)$ over the PDF of the SED output SNR, i.e., $\overline{P}_s = \int_0^{\infty} P_s(g) f_{g_{\rm sed}}(g)\, dg$, where $P_s(g)$ depends on the employed modulation scheme [1, Ch. 8]. By substituting (17) in the previous integral, the ASEP for multibranch SED receivers can be expressed as

$$\begin{aligned} \overline{P}_s = & \sum_{i=0}^{L-1} \sum_{k_1,k_2,\ldots,k_U=0}^{\infty} p_i \xi_L^{\kappa_L} \mathcal{A}\left[\mathbf{\Sigma}_{\mathbf{g}^{(i,L-1)}}, \{k_u\}_{u=1}^{U}\right] \\ & \times \mathcal{C}_{L-1}(g_T) \Upsilon(\kappa_L, \xi_L) \\ & + \sum_{i=0}^{L-1} \left\{ p_i \frac{(m/\overline{g})^m}{\Gamma(m)} \Phi\left(m, \frac{m}{\overline{g}}\right) \right. \\ & \quad + \sum_{s=1}^{L-1} \sum_{k_1,k_2,\ldots,k_U=0}^{\infty} p_{(i-s)_L} \xi_{s+1}^{\kappa_{s+1}} \\ & \quad \left. \times \mathcal{A}\left[\mathbf{\Sigma}_{\mathbf{g}^{(i,s)}}, \{k_u\}_{u=1}^{U}\right] \mathcal{C}_s(g_T) \Phi(\kappa_{s+1}, \xi_{s+1}) \right\} \end{aligned} \tag{21}$$

where $\Upsilon(a,b) = \int_0^{g_T} P_s(g) H(a,b,g)\, dg$ and $\Phi(a,b) = \int_{g_T}^{\infty} P_s(g) H(a,b,g)\, dg$.

$$f_{g_{\rm sed}}(g) = \begin{cases} \frac{(1-\sqrt{\rho})^m}{\Gamma(m)} \sum_{i=0}^{L-1} \sum_{k_1,k_2,\ldots,k_L=0}^{\infty} \frac{p_i \Gamma\left(m + \sum_{j=1}^{L} k_j\right) \rho^{1/2 \sum_{j=1}^{L} k_j} m^{k_L+m}}{\left[1+(L-1)\sqrt{\rho}\right]^{m+\sum_{j=1}^{L} k_j} \left[\overline{g}_i(1-\sqrt{\rho})\right]^{k_L+m} \prod_{j=1}^{L} k_j! \Gamma(k_j+m)} \\ \quad \times \prod_{j=1}^{L-1} \gamma\left[k_j + m, \frac{m g_T}{\overline{g}_{(i+j-L)_L}(1-\sqrt{\rho})}\right] g^{k_L+m-1} \exp\left[-\frac{mg}{\overline{g}_i(1-\sqrt{\rho})}\right], & g < g_T \\ \sum_{i=0}^{L-1} \left\{ p_i \frac{(m/\overline{g}_i)^m}{\Gamma(m)} g^{m-1} \exp\left(-\frac{mg}{\overline{g}_i}\right) + \frac{(1-\sqrt{\rho})^m}{\Gamma(m)} \right. \\ \quad \times \sum_{s=1}^{L-1} \sum_{k_1,k_2,\ldots,k_{s+1}=0}^{\infty} \frac{p_{(i-s)_L} \Gamma\left(m + \sum_{j=1}^{s+1} k_j\right) \rho^{1/2 \sum_{j=1}^{s+1} k_j} m^{k_{s+1}+m}}{(1+s\sqrt{\rho})^{m+\sum_{j=1}^{s+1} k_j} \left[\overline{g}_i(1-\sqrt{\rho})\right]^{k_{s+1}+m} \prod_{j=1}^{s+1} k_j! \Gamma(k_j+m)} \\ \quad \left. \times \prod_{j=1}^{s} \gamma\left[k_j + m, \frac{m g_T}{\overline{g}_{(i+j-s-1)_{s+1}}(1-\sqrt{\rho})}\right] g^{k_{s+1}+m-1} \exp\left[-\frac{mg}{\overline{g}_i(1-\sqrt{\rho})}\right] \right\}, & g \geq g_T \end{cases} \tag{19}$$

TABLE I
$N_{\min}$ REQUIRED IN (20) WITH $L = 3$ FOR CONVERGENCE OF THE OP P_{out} FOR $g_T = -10$ dB, $\overline{g}_1 = 0$ dB, AND $e_{\text{rel}} \leq 10^{-6}$

	Con-CM, $\rho = 0.1$				Lin-CM			
g_{th} (dB)	$m = 1.0$	$m = 1.5$	$m = 2.0$	$m = 4.0$	$m = 1.0$	$m = 1.5$	$m = 2.0$	$m = 4.0$
5	3	3	4	4	4	5	6	7
0	2	3	3	4	3	5	5	6
-5	2	2	3	3	3	4	4	5
-10	2	2	2	3	2	2	2	3
-15	1	2	2	2	2	2	2	2
-20	1	1	2	2	1	1	2	2

For example, for binary differential phase-shift keying (BDPSK) and M-ary noncoherent frequency-shift keying (M-NFSK),[2] $P_s(g) = \lambda \exp(-\mu g)$, with λ and μ being constants. Thus, using [29, eq. (8.381/1)] and [29, eq. (8.381/3)] yields

$$\Upsilon(a,b) = \lambda(\mu+b)^{-a}\gamma\left[a,(\mu+b)g_T\right] \tag{22a}$$

$$\Phi(a,b) = \lambda(\mu+b)^{-a}\Gamma\left[a,(\mu+b)g_T\right] \tag{22b}$$

respectively. For other modulation schemes, such as quadrature phase shift keying (QPSK) and square M-ary quadrature amplitude modulation (M-QAM), $P_s(g) = \lambda \text{erfc}(\sqrt{\mu g})$, where $\text{erfc}(\cdot)$ is the complementary error function [29, eq. (8.250/4)]. For these modulation schemes, $\Upsilon(a,b)$ and $\Phi(a,b)$ used in (21) can easily be expressed in closed form for integer values of m using [12, eq. (7)] and [12, eq. (10)] as

$$\Upsilon(a,b) = \lambda\frac{\Gamma(a)}{b^a}\left[1 - \sqrt{\frac{\mu}{b+\mu}}\sum_{k=0}^{m-1} c_k \left(\frac{b}{b+\mu}\right)^k\right] - \Phi(a,b) \tag{23a}$$

$$\Phi(a,b) = \lambda\frac{\Gamma(a)}{b^a}\left\{\text{erfc}(\sqrt{\mu g_T})\frac{\Gamma(a,bg_T)}{\Gamma(a)} - \sqrt{\frac{\mu}{\pi}}\sum_{k=0}^{m-1}\frac{b^k\Gamma\left[k+1/2,(b+\mu)g_T\right]}{(b+\mu)^{k+1/2}\Gamma(k+1)}\right\} \tag{23b}$$

respectively, where $c_1 = 0$ and $c_k = (2k-1)c_{k-1}/2k$ for $k = 1, 2, \ldots, m-1$ [31].

By substituting (9) and (10) in (21), an analytical expression for the exact $\overline{P}_s$ for constantly correlated multibranch SED receivers is obtained as in (24), shown at the bottom of the page. Similarly, substituting (11)–(14) in (21) yields an analytical expression for the exact $\overline{P}_s$ for arbitrarily correlated triple-branch SED receivers. For $L \geq 4$ and arbitrarily correlated i.d. fading, substituting (11)–(14) in (21) and (15) and (16) with $\mathbf{Z} = \mathbf{W}_{\mathbf{g}^{(i,n)}}$ when $\mathbf{W}_{\mathbf{g}^{(i,n)}}$ is tridiagonal and with $\mathbf{Z} = \mathbf{C}^{-1}_{\mathbf{g}^{(i,n)}}$ for arbitrary forms of $\mathbf{W}_{\mathbf{g}^{(i,n)}}$'s yields an analytical approximation for the exact $f_{g_{\text{sed}}}(g)$. Due to space limitations, the latter two expressions are not presented here but are available in [28].

In principle, the optimum g_T, i.e., g_T^*, that minimizes $\overline{P}_s$ can be obtained by solving $\vartheta\overline{P}_s/\vartheta g_T|_{g_T = g_T^*} = 0$. However, it is extremely difficult, if not impossible, to derive an analytical expression for g_T^*. Values for g_T^* can be found by employing root-finding analytical techniques that are available as built-in functions in well-known mathematical software packages, such as MATHEMATICA.

IV. PERFORMANCE EVALUATION RESULTS AND DISCUSSION

The analytical expressions of the previous section have been used to evaluate the performance of the multibranch SED receivers under consideration. Furthermore, equivalent performance evaluation results obtained by means of Monte Carlo simulations will also be presented. For the CM $\mathbf{\Sigma}_{\mathbf{g}^{(L-1,L-1)}}$, the following correlations have been considered: 1) uncorrelated CM (Unc-CM), where $\mathbf{\Sigma}_{\mathbf{g}^{(L-1,L-1)}} = \mathbf{I}_L$, with $\mathbf{I}_L$ being the $L \times L$ identity matrix; 2) linear CM (Lin-CM), where, for $L = 3$ and 4, $\mathbf{\Sigma}_{\mathbf{g}^{(2,2)}}$ and $\mathbf{\Sigma}_{\mathbf{g}^{(3,3)}}$ are given by [16, eq. (38)] and [25, eq. (14)], respectively; 3) triangular CM (Tri-CM), with $\mathbf{\Sigma}_{\mathbf{g}^{(2,2)}}$ given by [16, eq. (37)]; and 4) constant CM (Con-CM), where $\mathbf{\Sigma}^{j,k}_{\mathbf{g}^{(L-1,L-1)}} = \rho$ for $j \neq k$. Moreover, for the performance-evaluation results, we have considered an exponential power decaying profile (PDP) $\overline{g}_\ell = \overline{g}_1 \exp[-\delta(\ell-1)]$, with δ being the power decaying factor. Clearly, wherever i.d. branches are considered, $\delta = 0$, and $\overline{g}_\ell = \overline{g}\ \forall\, \ell$.

Exact numerical evaluation of (20) and (21) requires summation of an infinite number of terms. However, in practice, a minimum number of terms are selected, leading to a certain accuracy. Setting equal summation terms $N_u = N_{\min}\ \forall\, u$ in (20), Table I shows the values of $N_{\min}$ required for the P_{out} with $L = 3$ to converge with relative error $e_{\text{rel}} \leq 10^{-6}$, compared with the P_{out} performance obtained by means

[2]It is noted that, for modulation order $M > 2$, Gray encoding is assumed so that $\overline{P}_s = \overline{P}_b \log_2(M)$, where $\overline{P}_b$ is the average bit error probability (ABEP).

$$\begin{aligned}
\overline{P}_s = {} & \frac{(1-\sqrt{\rho})^m}{\Gamma(m)}\sum_{i=0}^{L-1}\sum_{k_1,k_2,\ldots,k_L=0}^{\infty}\frac{p_i\Gamma\left(m+\sum_{j=1}^{L}k_j\right)\rho^{1/2\sum_{j=1}^{L}k_j}}{\left[1+(L-1)\sqrt{\rho}\right]^{m+\sum_{j=1}^{L}k_j}\prod_{j=1}^{L}k_j!\Gamma(k_j+m)}\left[\frac{m}{\overline{g}_i(1-\sqrt{\rho})}\right]^{k_L+m} \\
& \times\prod_{j=1}^{L-1}\gamma\left[k_j+m,\frac{mg_T}{\overline{g}_{(i+j-L)_L}(1-\sqrt{\rho})}\right]\Upsilon\left[k_L+m,\frac{m}{\overline{g}_i(1-\sqrt{\rho})}\right] \\
& +\sum_{i=0}^{L-1}\left\{p_i\frac{(m/\overline{g})^m}{\Gamma(m)}\Phi\left(m,\frac{m}{\overline{g}}\right)+\frac{(1-\sqrt{\rho})^m}{\Gamma(m)}\sum_{s=1}^{L-1}\sum_{k_1,k_2,\ldots,k_{s+1}=0}^{\infty}p_{(i-s)_L}\right. \\
& \left.\times\frac{\rho^{1/2\sum_{j=1}^{s+1}k_j}\Gamma\left(m+\sum_{j=1}^{s+1}k_j\right)}{(1+s\sqrt{\rho})^{m+\sum_{j=1}^{s+1}k_j}\prod_{j=1}^{s+1}k_j!\Gamma(k_j+m)}\left[\frac{m}{\overline{g}_i(1-\sqrt{\rho})}\right]^{k_{s+1}+m}\Phi\left[k_{s+1}+m,\frac{m}{\overline{g}_i(1-\sqrt{\rho})}\right]\right\}
\end{aligned} \tag{24}$$

TABLE II
$N_{\min}$ REQUIRED IN (21) USING (9) AND (10) WITH $L = 4$ FOR CONVERGENCE OF THE ABEP $\overline{P}_b$ OF BDPSK FOR $g_T = 10$ dB AND $e_{\text{rel}} \leq 10^{-6}$

	Con-CM, $\rho = 0.2$				Con-CM, $\rho = 0.8$			
$\overline{g}_b$ (dB)	$m = 1.0$	$m = 2.0$	$m = 3.0$	$m = 4.0$	$m = 1.0$	$m = 2.0$	$m = 3.0$	$m = 4.0$
-5	18	18	20	21	34	49	68	72
0	15	16	18	19	29	35	48	61
5	12	15	15	17	23	18	31	42
10	5	7	7	8	2	15	17	22
15	2	2	2	2	6	9	10	11

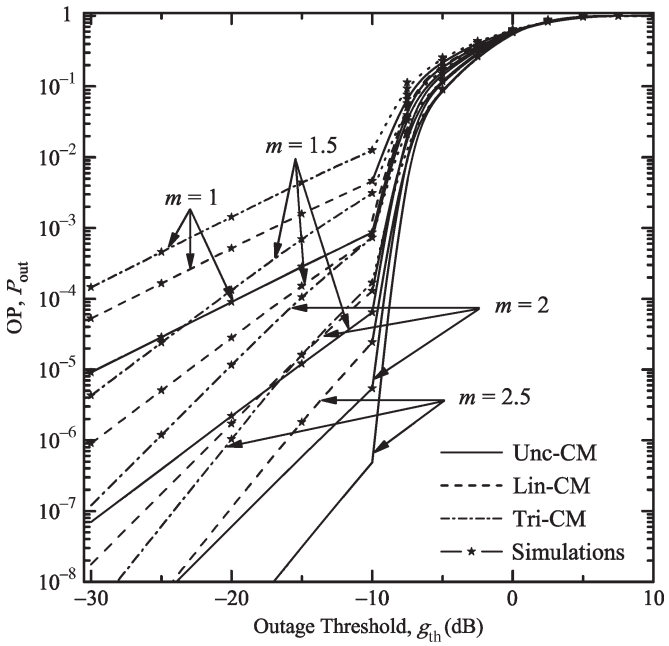

Fig. 1. OP P_{out} versus outage threshold g_{th} for triple-branch $(L = 3)$ SED receivers with $\overline{g}_1 = 0$ dB, $g_T = -10$ dB, and different values of m.

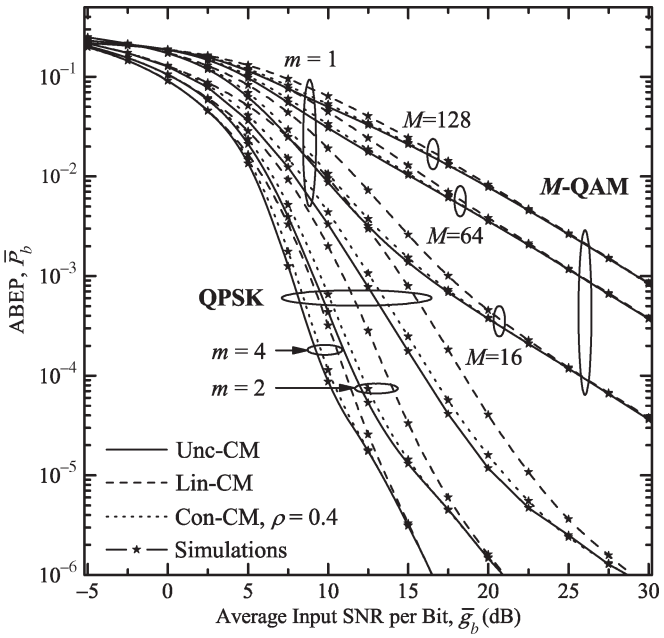

Fig. 2. ABEP $\overline{P}_b$ of QPSK and square M-QAM versus average input SNR per bit $\overline{g}_b$ for triple-branch $(L = 3)$ SED receivers with $g_T = 7$ dB and different values of m.

of computer simulations. We have considered a Con-CM with $\rho = 0.1$, a Lin-CM, various values of m and g_{th}, and an exponential PDP with $\delta = 0.2$, $\overline{g}_1 = 0$ dB, and $g_T = -10$ dB. It can be observed that $N_{\min}$ strongly depends on the outage threshold g_{th}. As g_{th} decreases, $N_{\min}$ also decreases, and for fixed g_{th}, $N_{\min}$ increases with increasing correlation and/or m. Furthermore, the convergence properties of (21) with (9) and (10) have been studied, considering again equal summation limits. Table II summarizes the values of $N_{\min}$ for the ABEP $\overline{P}_b$ (see footnote 2) of BDPSK with $L = 4$ to converge with relative error $e_{\text{rel}} \leq 10^{-6}$, compared with equivalent computer simulation performance results. Again, here, we have considered various values for m and for the average SNR per bit, $\overline{g}_b = \overline{g}/\log_2(M)$, Con-CMs with $\rho = 0.2$ and 0.8, and $g_T = 10$ dB. As summarized in Table II, with increasing $\overline{g}_b$, $N_{\min}$ will decrease, whereas, for fixed $\overline{g}_b$, $N_{\min}$ increases with increasing m and/or ρ. Additionally, the convergence behavior of (21) with (11)–(16) for $L = 4$ has been found to be similar to that observed for (21) with (9) and (10). Further experiments have shown that, to achieve certain accuracy, 1) $N_{\min}$ will increase for higher values of L, and 2) $N_{\min}$ seems independent of g_T.

Using (20), the P_{out} performance has been obtained as a function of g_{th}. Fig. 1 shows this performance for triple-branch SED receivers with an exponential PDP having $\delta = 0.1$, $\overline{g}_1 = 0$ dB, $g_T = -10$ dB, various correlations, and different values of m. As expected, P_{out} degrades with decreasing m and/or increasing g_{th} and/or increasing any of the correlation coefficients. Complementary computer simulated performance evaluation results have verified the accuracy of the analysis. The $\overline{P}_b$ versus $\overline{g}_b$ and/or g_T has been obtained by numerically evaluating (21) using (9)–(16) and is shown in Figs. 2–5 for different modulation formats, correlation models, and various values of m. In these figures, complementary performance evaluation results obtained by means of computer simulations are also included again, verifying the accuracy of the analytical expressions derived for $L \leq 3$, as well as approximations for $L \geq 4$. As shown in Fig. 2 for $L = 3$ and $g_T = 7$ dB, the $\overline{P}_b$ of QPSK and M-QAM improves with increasing $\overline{g}_b$ and m, and the impact of branch correlation on $\overline{P}_b$ becomes more severe as m increases. It is also evident that, under severe fading conditions and for fixed $\overline{g}_b$, the $\overline{P}_b$ degradation due to correlated fading increases with decreasing M. Fig. 3 shows the $\overline{P}_b$ of BDPSK versus g_T for $L = 3$ and $\overline{g}_b = 20$ dB. It also shows the existence of an optimal g_T, i.e., g_T^*, that minimizes $\overline{P}_b$, and its specific value depends on m and/or the receiver's CM. In Figs. 4 and 5, the $\overline{P}_b$ performance of BDPSK for triple-branch SED and SSD, as well as quadruple-branch SED, is plotted versus $\overline{g}_b$, considering, for all cases, the optimal value of g_T, i.e., g_T^*. The trend of these performance evaluation results is similar to the case of SED with QPSK and M-QAM signals (see Fig. 2). In other words, for both diversity techniques, the $\overline{P}_b$ of BDPSK improves with increasing $\overline{g}_b$ and m. Furthermore, as m increases, $\overline{P}_b$ improves when the value of any of the correlation coefficients decreases. In addition, it is evident from Fig. 4 that, even under highly correlated and severe fading conditions, triple-branch SED outperforms uncorrelated SSD with this performance improvement increasing as $\overline{g}_b$ increases. As shown in Fig. 5, increasing L improves the $\overline{P}_b$ performance for every correlation under consideration, although it increases the impact of correlation on $\overline{P}_b$, compared with similar performance results shown

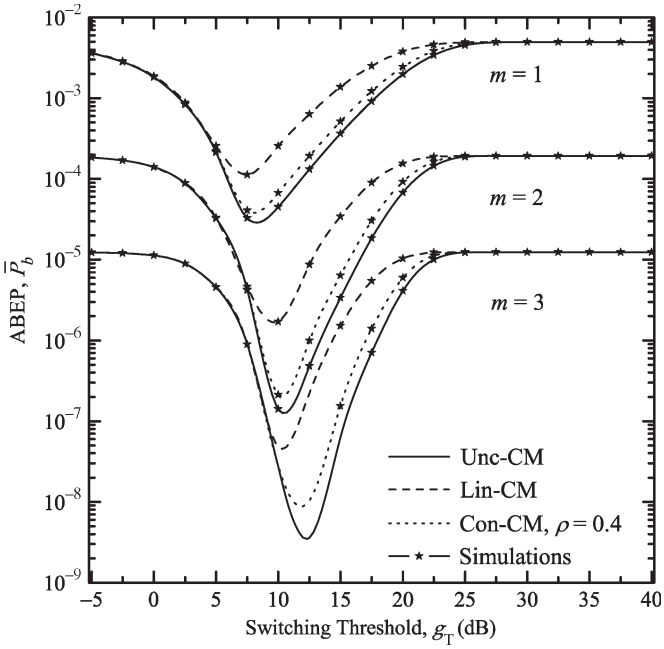

Fig. 3. ABEP $\overline{P}_b$ of BDPSK versus switching threshold g_T for triple-branch $(L = 3)$ SED receivers with $\overline{g}_b = 20$ dB and different values of m.

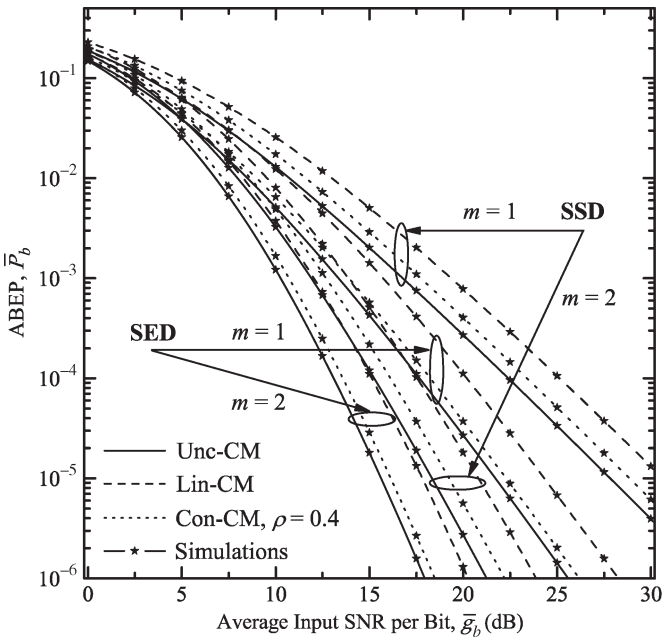

Fig. 4. ABEP $\overline{P}_b$ of BDPSK versus average input SNR per bit $\overline{g}_b$ for triple-branch $(L = 3)$ SSD and SED receivers with g_T^* and different values of m.

in Fig. 4. It is finally noted that similar conclusions for the $\overline{P}_b$ as those obtained from Figs. 2–5 for specific modulation formats have been found for other modulations, such as M-ary PSK (M-PSK), M-ary differential PSK (M-DPSK), and M-NFSK.

V. Conclusion

Digital signal reception with multibranch SED over arbitrarily correlated and not necessarily i.d. Nakagami-m fading channels has been studied. For the constant correlation model, analytical expressions for the exact distribution of the multibranch SED output SNR have been obtained. For the most general case of arbitrary correlation and for half-integer or integer values of m, analytical expressions and

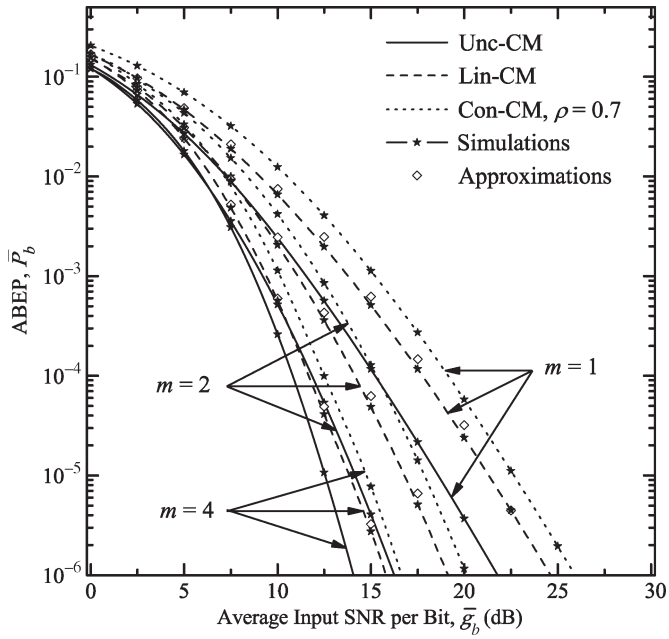

Fig. 5. ABEP $\overline{P}_b$ of BDPSK versus average input SNR per bit $\overline{g}_b$ for quadruple-branch $(L = 4)$ SED receivers with g_T^* and different values of m.

accurate approximations for the exact distribution of output SNR have been derived for up to three and more than three branches of SED, respectively. All derived exact expressions and approximations have further been used to study the OP and ASEP of multibranch SED receivers. Numerically evaluated performance results compared with equivalent computer simulation results have verified the presented analysis.

Acknowledgment

The authors would like to thank all five reviewers and the editor for their constructive comments, which helped in the improvement of the quality of our paper.

References

[1] M. K. Simon and M.-S. Alouini, *Digital Communication Over Fading Channels,* 2nd ed. New York: Wiley, 2005.

[2] M. A. Blanco and K. J. Zdunek, "Performance and optimization of switched diversity systems for the detection of signals with Rayleigh fading," *IEEE Trans. Commun.*, vol. COM-27, no. 12, pp. 1887–1895, Dec. 1979.

[3] A. A. Abu-Dayya and N. C. Beaulieu, "Analysis of switched diversity systems on generalized-fading channels," *IEEE Trans. Commun.*, vol. 42, no. 12, pp. 2959–2966, Nov. 1994.

[4] H.-C. Yang and M.-S. Alouini, "Performance analysis of multibranch switched diversity systems," *IEEE Trans. Commun.*, vol. 51, no. 5, pp. 782–794, May 2003.

[5] H.-C. Yang and M.-S. Alouini, "Markov chains and performance comparison of switched diversity systems," *IEEE Trans. Commun.*, vol. 52, no. 7, pp. 1113–1125, Jul. 2004.

[6] H.-C. Yang and M.-S. Alouini, "Generalized switch-and-examine combining (GSEC): A low-complexity combining scheme for diversity-rich environments," *IEEE Trans. Commun.*, vol. 52, no. 10, pp. 1711–1721, Oct. 2004.

[7] H.-C. Yang and M.-S. Alouini, "Improving the performance of switched diversity with post-examining selection," *IEEE Trans. Wireless Commun.*, vol. 5, no. 1, pp. 67–71, Jan. 2006.

[8] H.-C. Yang, M. K. Simon, and M.-S. Alouini, "Scan and wait combining (SWC): A switch and examine strategy with a performance-delay tradeoff," *IEEE Trans. Wireless Commun.*, vol. 5, no. 9, pp. 2477–2483, Sep. 2006.

[9] M.-S. Alouini and H.-C. Yang, "Minimum estimation and combining generalized selection combining (MEC-GSC)," *IEEE Trans. Wireless Commun.*, vol. 6, no. 2, pp. 526–532, Feb. 2007.

[10] C. Tellambura, A. Annamalai, and V. K. Bhargava, "Unified analysis of switched diversity systems in independent and correlated fading channels," *IEEE Trans. Commun.*, vol. 49, no. 11, pp. 1955–1965, Nov. 2001.
[11] G. Femenias, "Reference-based dual switched and stay diversity systems over correlated Nakagami fading channels," *IEEE Trans. Veh. Technol.*, vol. 52, no. 4, pp. 902–918, Jul. 2003.
[12] L. Xiao and X. Dong, "New results on the BER of switched diversity combining over Nakagami fading channels," *IEEE Commun. Lett.*, vol. 9, no. 2, pp. 136–138, Feb. 2005.
[13] N. Maleki, E. Karami, and M. Shiva, "Optimization of antenna array structures in mobile handsets," *IEEE Trans. Veh. Technol.*, vol. 54, no. 4, pp. 1346–1351, Jul. 2005.
[14] S. Wei, D. Goeckel, and R. Janaswamy, "On the capacity of MIMO systems with antenna arrays of fixed volume," *IEEE Trans. Wireless Commun.*, vol. 4, no. 4, pp. 1608–1621, Jul. 2005.
[15] C. C. Tan and N. C. Beaulieu, "Infinite series representations of the bivariate Rayleigh and Nakagami-m distributions," *IEEE Trans. Commun.*, vol. 45, no. 10, pp. 1159–1161, Oct. 1997.
[16] Q. T. Zhang, "Maximal-ratio combining over Nakagami fading channels with an arbitrary branch covariance matrix," *IEEE Trans. Veh. Technol.*, vol. 48, no. 4, pp. 1141–1150, Jul. 1999.
[17] R. K. Mallik, "On multivariate Rayleigh and exponential distributions," *IEEE Trans. Inf. Theory*, vol. 49, no. 6, pp. 1499–1515, Jun. 2003.
[18] G. K. Karagiannidis, D. A. Zogas, and S. A. Kotsopoulos, "On the multivariate Nakagami-m distribution with exponential correlation," *IEEE Trans. Commun.*, vol. 51, no. 8, pp. 1240–1244, Aug. 2003.
[19] G. K. Karagiannidis, D. A. Zogas, and S. A. Kotsopoulos, "An efficient approach to multivariate Nakagami-m distribution using Green's matrix approximation," *IEEE Trans. Wireless Commun.*, vol. 2, no. 5, pp. 883–889, Sep. 2003.
[20] Y. Chen and C. Tellambura, "Performance analysis of three-branch selection combining over arbitrarily correlated Rayleigh-fading channels," *IEEE Trans. Wireless Commun.*, vol. 4, no. 3, pp. 861–865, May 2005.
[21] Y. Chen and C. Tellambura, "Infinite series representation of the trivariate and quadrivariate Rayleigh distribution and their applications," *IEEE Trans. Commun.*, vol. 53, no. 12, pp. 2092–2101, Dec. 2005.
[22] P. Dharmawansa, N. Rajatheva, and C. Tellambura, "Infinite series representations of the trivariate and quadrivariate Nakagami-m distributions," *IEEE Trans. Wireless Commun.*, vol. 6, no. 12, pp. 4320–4328, Dec. 2007.
[23] P. S. Bithas and P. T. Mathiopoulos, "Performance analysis of SSC diversity receivers over correlated Ricean fading satellite channels," *EURASIP J. Wireless Commun. Netw.*, vol. 2007, no. 1, Jan. 2007, Art. ID 25361, 9 p.
[24] P. S. Bithas, N. C. Sagias, and P. T. Mathiopoulos, "Dual diversity over correlated Ricean fading channels," *J. Commun. Netw.*, vol. 9, no. 1, pp. 67–74, Mar. 2007.
[25] G. C. Alexandropoulos, N. C. Sagias, F. I. Lazarakis, and K. Berberidis, "New results for the multivariate Nakagami-m fading model with arbitrary correlation matrix and applications," *IEEE Trans. Wireless Commun.*, vol. 8, no. 1, pp. 245–255, Jan. 2009.
[26] J. Reig, "Multivariate Nakagami-m distribution with constant correlation model," *Int. J. Electron Commun. (AEU)*, vol. 63, no. 1, pp. 46–51, Jan. 2009.
[27] K. Peppas and N. C. Sagias, "A trivariate Nakagami-m distribution with arbitrary covariance matrix and applications to generalized selection diversity receivers," *IEEE Trans. Commun.*, vol. 57, no. 7, pp. 1896–1902, Jul. 2009.
[28] G. C. Alexandropoulos, "Performance analysis of multichannel receivers over correlated fading channels," Ph.D. dissertation, Univ. Patras, Patras, Greece, Jun. 2010, to be published.
[29] I. S. Gradshteyn and I. M. Ryzhik, *Table of Integrals, Series, and Products,* 6th ed. New York: Academic, 2000.
[30] A. S. Krishnamoorthy and M. Parthasarathy, "A multivariate gamma-type distribution," *Ann. Math. Statist.*, vol. 22, no. 4, pp. 549–557, Dec. 1951.
[31] D. B. Owen, "A table of normal integrals," *Commun. Statist.-Simul. Comput.*, vol. 9, no. 4, pp. 389–419, Oct. 1980.

A Hybrid Architecture for Delay Analysis of Interleaved FEC on Mobile Platforms

Kyungtae Kang, *Member, IEEE*, Cheolgi Kim, *Member, IEEE*, and Kyung-Joon Park, *Member, IEEE*

***Abstract*—Forward error correction (FEC) is the preferred way of coping with the error-prone nature of wireless links in broadcasting systems, because it can provide a bounded delay, which is a particular consideration for real-time multimedia applications. Additionally, controlling the variability of the delay, or jitter, is important in achieving seamless multimedia services. We show that error control using Reed–Solomon (RS) FEC in the medium-access control (MAC) layer can be a major source of jitter. We predict the expected delay incurred by RS decoding for varying levels of block interleaving in a mobile, under a range of channel conditions, using a hybrid simulation and analytic approach, which is based on the error statistics of data transmission over fading channels. The results allow us to determine the size of the buffer required to avoid frequent service interruptions.**

***Index Terms*—Delay estimation, hybrid architecture, interleaved forward error correction (FEC), mobile systems.**

I. Introduction

Broadcast and multicast services in CDMA2000 wireless networks [1], [2] can simultaneously provide uniform high-quality multimedia to a large number of subscribers. For this purpose, an outer forward error-correction (FEC) code in the medium-access control (MAC) layer is used in combination with the physical-layer inner turbo code [3]. This combination enhances the transmission efficiency, irrespective of any explicit power control. The CDMA2000 air specification [4] states that Reed–Solomon (RS) codes with the coding rates of 12/16, 13/16, and 14/16 should be considered as the options for the outer code, owing to their superior performance at low error rates [5]–[7].

An RS code is specified by a tuple (N, K), where K and $(N - K)$ are the number of information bytes and parity bytes, respectively, in each codeword. The RS algebraic erasure decoding procedure is then able to correct up to $(N - K)$ damaged bytes, which are located by a cyclic redundancy check in the physical layer, in each RS codeword. The physical-layer protocol erases these damaged bytes and informs the RS erasure decoder of their locations.

Before applying RS encoding, the access network transfers the data, which consists of broadcast security packets [4], into a buffer called an error control block (ECB) for each logical channel. The data are entered into the ECB row by row, RS coding is applied to the columns of the ECB, and the access network transmits the data from the ECB on the broadcast channel, again by row. Each row of an ECB constructs M broadcast MAC packets, and each of these packets contains 125 B of the ECB as its payload, together with a 2-bit MAC trailer. The

Manuscript received June 24, 2009; revised September 30, 2009. First published January 15, 2010; current version published May 14, 2010. This work was supported by the Korean Government Ministry of Education and Human Resources Development under Korea Research Foundation Grant KRF-2007-357-D00174. The review of this paper was coordinated by Prof. C. P. Oestges.

The authors are with the Thomas M. Siebel Center for Computer Science, Department of Computer Science, University of Illinois at Urbana-Champaign, Urbana, IL 61801-2302 USA (e-mail: ktkang@illinois.edu; cheolgi@illinois.edu; kjp@illinois.edu).

Color versions of one or more of the figures in this paper are available online at http://ieeexplore.ieee.org.

Digital Object Identifier 10.1109/TVT.2010.2040640